

Fatigue Crack Growth Path of 2324-T39 Aluminium Alloy under Constant-Amplitude and Spectrum Tension Loading

BAO Rui¹, ZHANG Ting², FEI Binjun³

¹ Institute of Solid Mechanics, School of Aeronautic Science and Engineering, Beihang University, Beijing, P.R. China, 100191, rbao@buaa.edu.cn

² zhangting19860811@163.com

³ feibj@buaa.edu.cn

ABSTRACT. A study has been accomplished to characterize the fatigue crack growth path in aluminum alloy 2324-T39 L-T oriented middle tension specimen under constant amplitude (CA) and simple variable amplitude (VA) loading conditions. The effect of stress intensity factor ranges (ΔK -levels), stress ratios (R), overloads and underloads on crack growth path are examined. The test results indicate that: 1) Crack meandering and/or branching appeared in both CA and VA loading conditions; 2) ΔK -level tends to be the dominant factor on crack path deviation, while R ratios show little effect on the changing of crack growth path for this alloy; 3) Cracks bifurcation appeared in the VA loading conditions is resulted from the linkage of secondary surface crack and the main crack, irrespective to the interval of peak load and the existence of underloads.

INTRODUCTION

Aluminum Alloy (AA) 2324 is one of the representative Al-Cu-Mg alloys developed by Alcoa. 2324-T39 plate is a higher strength version of alloy 2024-T351 and is a high-purity controlled composition variant of alloy 2024. It was developed for tension-dominated, fatigue and fracture, critical plate applications, and has been used successfully on lower wing skin and center wing box components of new commercial transport aircrafts [1].

It is a common consensus that through thickness crack in metal plate subjected to tension load only is typical Mode I crack which tends to propagate straightly and perpendicular to the load direction. However, significant crack meandering or branching was observed during the crack growth tests on standard middle tension, M(T), specimens in L-T orientation of AA 2324-T39 under truncated flight-by-flight spectrum loading, which was reported in [2]. Apart from the metallurgical factors, loading condition, such as multi-axial loading [3], spectrum loading [4, 5] etc., and changes in configuration along the crack path, are considered to be factors which will lead to macro-level crack path deflection. For better understanding effect of load factors, i.e. stress ratio (R), stress intensity factor range (ΔK), tension overload and underloads, on

the crack growth path of AA 2324-T39 under tension dominated load condition, experimental investigations were performed and reported in this paper.

EXPERIMENTS

Material and Specimen

The chemical composition data of 2324 is found in reference [1]: (WT%), Si 0.1, Fe 0.12, Cu 3.8~4.4, Mn 0.3~0.9, Mg 1.2~1.8, Cr 0.10, Zn 0.25, Ti 0.15, others each 0.05, others total 0.15, aluminium remainder. The mechanical properties are also available in [1], i.e. tensile strength 475 MPa, yield strength 370 MPa, elongation 8%, K_{IC} values for thin plate (19.05~33.02mm) L-T 38.5~44 MPa \sqrt{m} .

The fatigue crack growth (FCG) tests in this study were conducted using M(T) specimens. The dimensions of the specimen are given in Fig.1. All the specimens are in L-T orientation, i.e. the applied external load is along the longitudinal (rolling) direction and the crack propagates along the transverse direction.

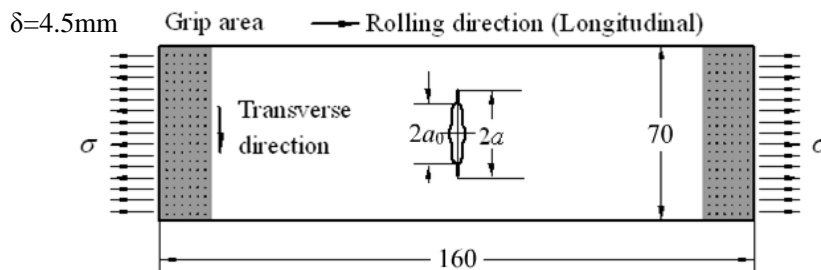


Figure 1. M(T) specimens principal dimensions (Unit: mm)

Experimental procedure

All the FCG tests were accomplished using Instron8803 servo hydraulic fatigue test system, and an observation system consisting of a digital microscope, a servo motor, and raster ruler is used to register the position of crack tip. Specimens were held in a pair of 100 mm wide hydraulic grip wedges.

Pre-cracking procedures were accomplished under constant amplitude load of $R = 0.06$ and $\sigma_{max} = 90$ MPa, which resulted in an initial half crack length of about 1 mm from the notch tip. The FCG tests were subsequently carried out under the selected loading conditions until the half crack length is greater than 18 mm or the crack advances arrested. All the tests were run in laboratory air.

Loading conditions

Three kinds of loading conditions were designed to investigate the effects of R ratios, ΔK -levels and overloads. The list of specimens and loading conditions in this study are in Table 1.

The first kind of loading conditions, stated as LC1, is constant amplitude (CA)

loading of two R ratios i.e. $R = 0.06$ and 0.5 . For $R = 0.06$, the maximum applied nominal stress $\sigma_{\max} = 90$ MPa and 170 MPa, and the resulted ΔK -levels is in $9\sim 35$ $\text{MPa}\sqrt{\text{m}}$. For $R = 0.5$, $\sigma_{\max} = 110$ MPa, and the ΔK values in $7\sim 17$ $\text{MPa}\sqrt{\text{m}}$.

The second kind of loading condition, stated as LC2, is obtained by adding a high peak load to LC1, see in Fig. 2(a). The CA loading is $R = 0.06$, $\sigma_{\max} = 110$ MPa, and the peak load is $\sigma_{\max} = 170$ MPa. The minimum loading in the spectrum is kept constant at the level of $\sigma_{\min} = 6.6$ MPa. Three intervals (n), cycles between two peak loads, i.e. $n = 2100$, 4200 and 8400 , are selected in this study.

The third kind of loading conditions, stated as LC3, which is slightly different from LC2, is achieved by adding a negative amplitude load, $\sigma_{\min} = -17$ MPa, also called underload, immediately after the overloads, see Fig. 2(b). The interval n is 4200 .

Table 1. Specimen and loading condition listing

Specimen ID	Load ratio(R)	Max K ($\text{MPa}\sqrt{\text{m}}$)	Max ΔK ($\text{MPa}\sqrt{\text{m}}$)	Crack Length at Max K (mm)	a_0 (mm)	Frequency (Hz)
LC1-0.06-90-1	0.06	24.0	22.5	16.6	2.0	10
LC1-0.06-90-2	0.06	25.5	24.0	17.8	2.0	10
LC1-0.06-90-3	0.06	26.4	24.8	18.5	2.0	10
LC1-0.06-170-1	0.06	33.1	31.1	10.7	2.0	5
LC1-0.06-170-2	0.06	37.4	35.1	12.9	2.0	5
LC1-0.5-110-1	0.5	27.6	13.8	15.4	2.0	5
LC1-0.5-110-2	0.5	33.2	16.6	19.0	2.0	5
LC2-2100-1	0.06	25.5	24.0	6.8	3.2	5
LC2-4200-1	0.06	31.0	29.0	9.4	2.0	5
LC2-4200-2	0.06	28.0	26.5	8.2	2.0	5
LC2-8400-1	0.06	36.8	34.6	12.6	3.2	5
LC2-8400-2	0.06	34.3	32.2	11.3	3.2	5
LC3-4200-1	0.06	24.5	23.0	6.3	2.0	5
LC3-4200-2	0.06	23.0	21.5	5.6	2.0	5

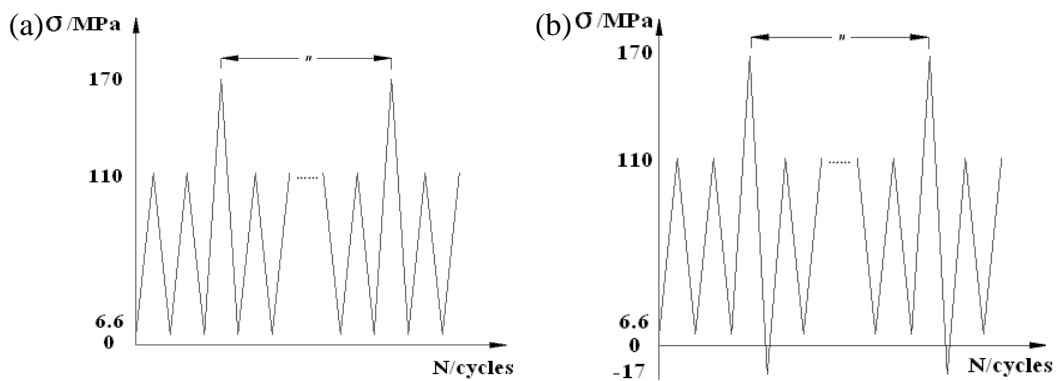


Figure 2. Constant amplitude loading with overloads and underloads

RESULTS AND DISCUSSION

Crack Path under LC1 – Effect of ΔK

There are three specimens, i.e. LC1-0.06-90-1, LC1-0.06-90-2, LC1-0.06-90-3, tested under the loading condition of $R = 0.06$, $\sigma_{\max} = 90$ MPa, which results in the ΔK values in the range of 9~24 $\text{MPa}\sqrt{\text{m}}$. Two specimens, i.e. LC1-0.06-170-1, LC1-0.06-170-2, tested under $R = 0.06$, $\sigma_{\max} = 170$ MPa with the ΔK values in the range of 19~35 $\text{MPa}\sqrt{\text{m}}$. The crack paths of the 5 specimens are shown in Fig. 3.

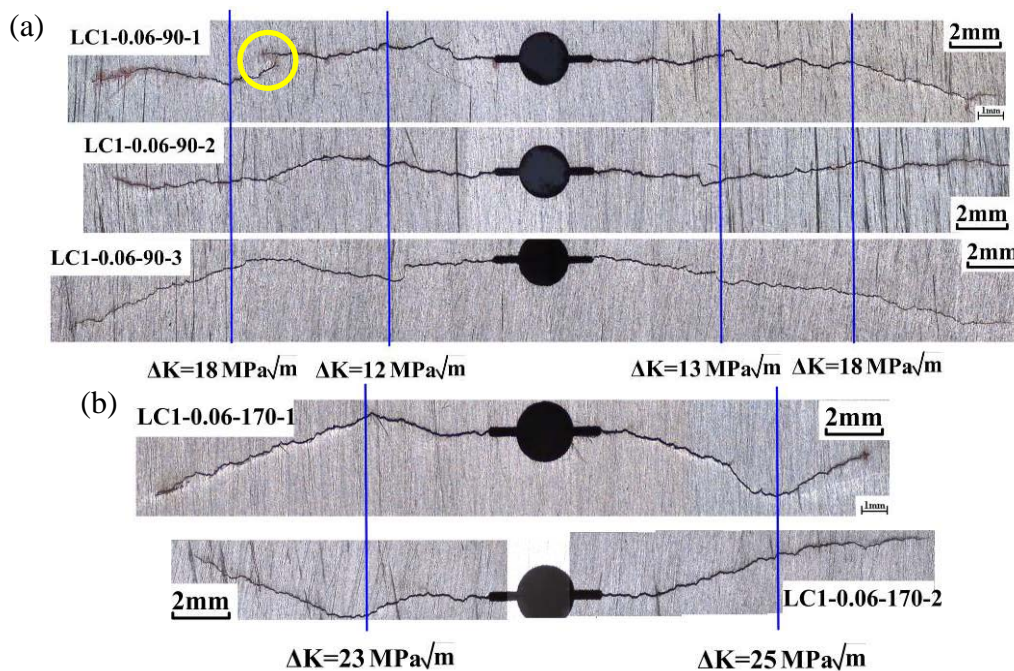


Figure 3. Crack paths of under CA loading of $R = 0.06$, $\sigma_{\max} = 90$ MPa for (a) and $\sigma_{\max} = 170$ MPa for (b)

Figure 3 indicates that (1) for the loading condition of $R = 0.06$, $\sigma_{\max} = 90$ MPa, ΔK values in 9~24 $\text{MPa}\sqrt{\text{m}}$, the crack growth paths in macro-level are much more ‘ideally’ compared with that of $\sigma_{\max} = 170$ MPa, though the crack paths show meandering to some extent. Small macro-level crack branching were observed when the corresponding ΔK increased about 16.5 $\text{MPa}\sqrt{\text{m}}$ in LC1-0.06-90-1, marked by circle in Fig. 3(a); (2) for the circumstance of $R = 0.06$, $\sigma_{\max} = 170$ MPa, ΔK in the range of 19~35 $\text{MPa}\sqrt{\text{m}}$, significant crack path deviations with the angle of about 100 ~135 degree were found in both the two specimens, see Fig. 3 (b). The crack lengths a at the turning point are about 6~8 mm, and the corresponding ΔK is about 22~26 $\text{MPa}\sqrt{\text{m}}$. (3) no remarkable crack bifurcations appeared in the crack path during the propagation, which is quite different from the crack path under LC2 and LC3.

Crack Path under LC1 – Effect of R

According to available achievements, the increase of stress ratio R tends to increase the probability of crack growth path changes [6], crack growth tests under high R -level of 0.5 were performed to investigate the R effect on crack path. The applied $\sigma_{\max} = 110$ MPa which results in the ΔK values in 7~17 MPa $\sqrt{\text{m}}$. The crack appearances are illustrated in Fig. 4. Synthesizing the test results of $R = 0.06$ and 0.5, shown in Fig. 3(a) and Fig. 4, crack paths are principally perpendicular to the load direction when ΔK is lower than 18 MPa $\sqrt{\text{m}}$, the increase of R ratios lead to insignificant changes on crack morphology. Crack path deviation was found in LC1-0.5-110-1 at about $\Delta K = 13$ MPa $\sqrt{\text{m}}$. Small crack branching was also observed at the final stage of crack growth in LC1-0.5-110-2, where ΔK is about 16.5 MPa $\sqrt{\text{m}}$, marked by circles in Fig. 4.

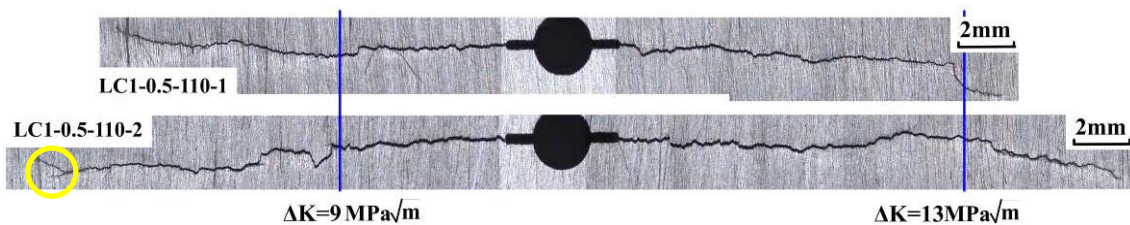


Figure 4. Crack paths of under CA loading of $R = 0.5$, $\sigma_{\max} = 110$ MPa

Crack Path under LC2 – Effect of Overloads

The effect of a single high load cycle on crack growth rate is abundantly studied, while, the effect of overloads on crack morphology is not well established. FCG tests under simple variable-amplitude (VA) loading history, i.e. CA loading with single peak load cycle in one block, were carried out to study the effect of overloads on crack path. Three intervals, $n = 2100$, 4200 and 8400, are selected. The tested crack paths are shown in Fig. 5. Both “static” fracture and retardation on cyclic propagation were observed when the crack suffered the peak load in the loading history.

For the case of the interval $n = 2100$ cycles, the results of which is given in Fig. 5(a), the main effect of overload on crack propagation is retardation. This effect becomes more and more serious with the increase of crack lengths, which leads to the fact that the propagation of the dominate crack is nearly arrested. The total increase in crack length during 30 blocks is about 3 mm. The static propagation of the crack when suffering the overload is not obvious. Crack branching was not observed immediately after the overloads. Surface secondary cracks were observed away from the growth path of the lead crack. The lead crack and the secondary cracks kept growing for a period of loading cycles until they were linked up, which has resulted in the observed branched crack. Crack branching appeared in both right and left sides of the specimens.

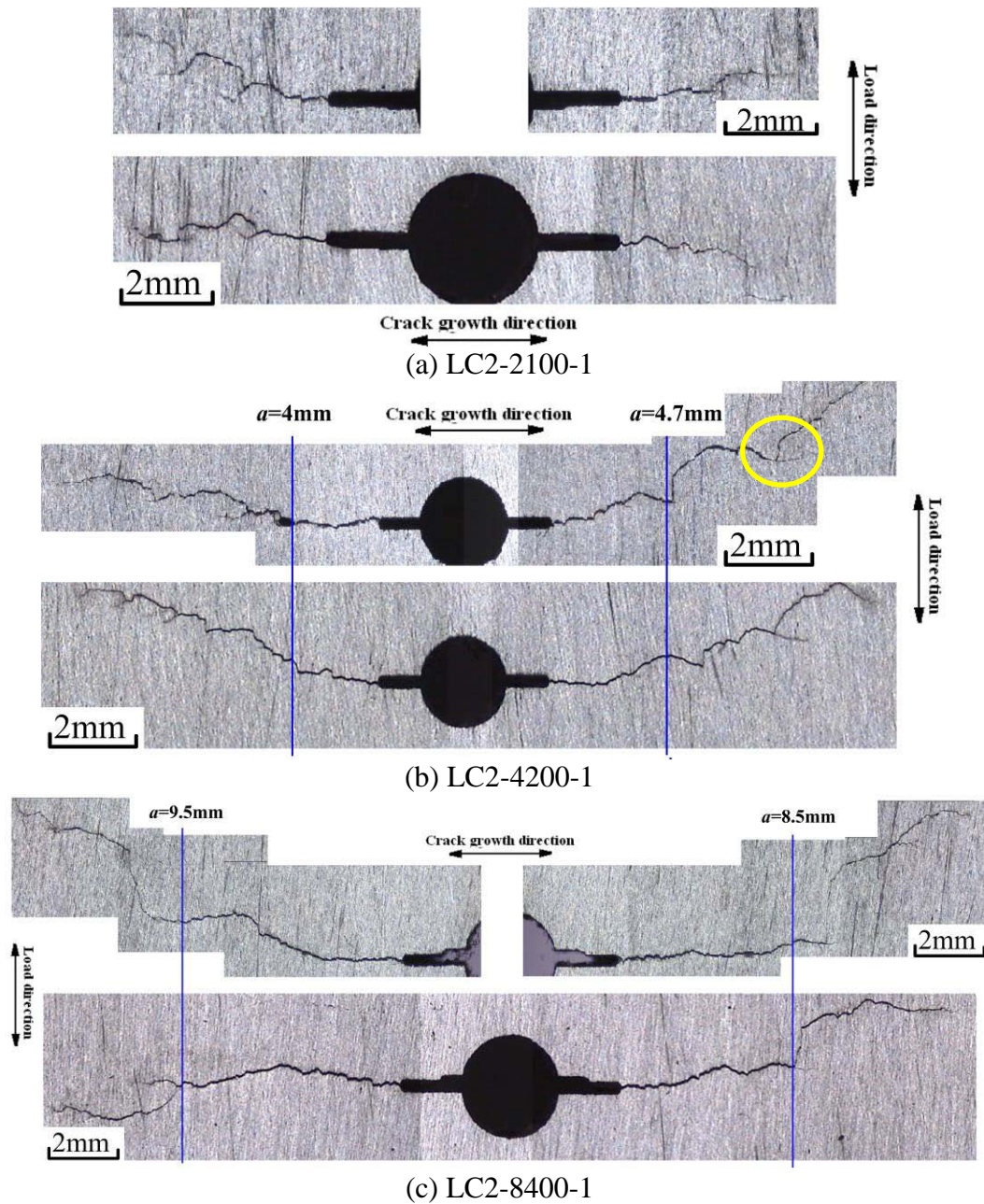


Figure 5. Crack Paths under LC2 of $n=2100$ for (a), $n=4200$ for (b) and $n=8400$ for (c)

For the case of the interval $n = 4200$ cycles, see Fig. 5(b), there is no significant macro-level crack branching when the crack length is limited within 4 mm. The increments in crack length due to static propagation, which is caused by the peak overload, and the cyclic growth, which is caused by the fatigue cycles between the two peak loads, are in the same order of magnitude. Significant crack growth retardation was observed right after the overload. Secondary surface cracks were found when the

crack length of the leading crack exceeds 5mm. The secondary crack and the main crack linked each other after several fatigue cycles. The crack growth rate of the secondary crack is much higher than that of the originally leading crack. The advancing of the originally leading crack tip is slowed down and arrested finally. New crack bifurcation appeared in the crack tip of the far branch of the crack. In consequence, the crack path of the new main crack tends to be far away from the horizontal axis. This procedure of crack growth is illustrated in Fig. 6, which is the point of crack bifurcation marked by circle in Fig. 5(b). Remarkable crack branching were found in both right and left sides of the crack and in both front and back of the specimen. The crack characteristics are similar in the two specimens tested under this loading condition, and similar to that under the high truncation level in Ref. [2].

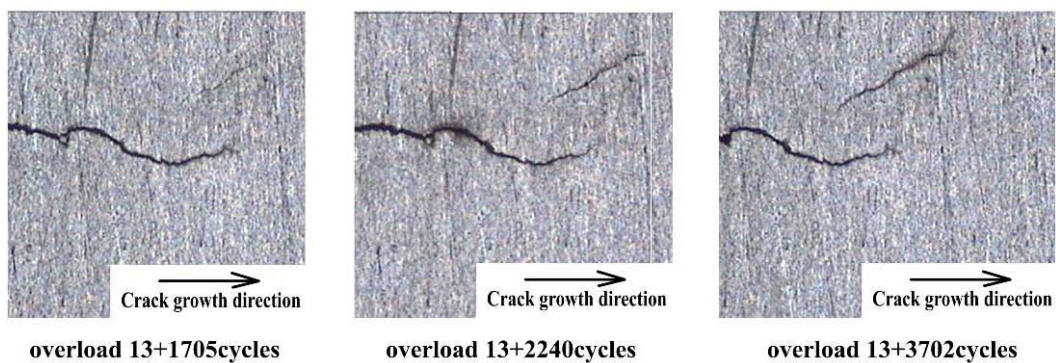


Figure 6. Propagation of the crack branches in LC2-4200-1

For the case of $n = 8400$ cycles, see Fig. 5(c), the crack bifurcation are not that serious compared with the crack path under the case of $n = 4200$ cycles. Especially for the part of crack length less than 8 mm, there is no significant crack branching in this stage. The increment in crack length due to cyclic growth is much larger than that due to the static propagation. There is a retardation in crack growth rate appears after the overload, however, the crack growth rate could recover to the rate level under CA loading condition before the arrival of the next peak load. Crack branchings were observed after the 4th peak load in the spectrum, at about $a = 9$ mm, on both sides of the crack. The advances of the new-appeared crack tips are much faster than that of the main crack, therefore, the crack paths deviate from the Mode I crack path.

Crack Path under LC3 – Effect of Overloads and Underloads

Studies on load interaction effects during fatigue crack growth under variable amplitude loading show that the large effect of the overloads will be drastically reduced if the overload innemately followed by an underloads [7]. For the loading condition LC3 in this study, i.e. a peak load $\sigma_{\max} = 170$ MPa followed by an underload of $\sigma_{\min} = -17$ MPa, interval between two peak loads $n = 4200$ cycles, the test results show contrary trend to the available achievements. The total crack length a of LC3-4200-1 is less than 7 mm after 25 LC3 blocks, however, the crack length in LC2-4200-1 has already exceed 9 mm

after 17 LC2 blocks. The crack morphology in LC3-4200-1 is more similar to that of LC2-2100-1, rather than LC2-4200-1.

SUMMARY AND CONCLUSIONS

Crack meandering and/or branching appeared in both CA and VA loading conditions for the aluminum alloy studied in this paper.

For the CA loading condition, no remarkable crack branching was observed, though the crack paths show meandering to some extent. Crack path deviation appears in high ΔK -level, the angles in crack trajectories are even exceed 100 degree at the ΔK -level of 22~26 MPa $\sqrt{\text{m}}$. R ratios show little effect on the changing of crack growth path of this alloy.

Significant crack branching was observed in VA loading condition irrespective of the interval of two peak loads. The crack bifurcation is resulted from the linkage of the main crack and the secondary surface cracks, which were observed away from the main crack paths. The advancing of the originally leading crack tip is slowed down and arrested finally. In consequence, the crack path of the new main crack tends to be far away from the horizontal axis. In terms of crack length, the branched crack appears earlier in the condition of $n = 2100$ than that of $n = 4200$, in consequence earlier than that of $n = 8400$. The reason is the competition between the plastic zone size and the crack increments due to static propagation and cyclic growth. The underloads following the peak load lead to little change in crack paths compare to that under the loading condition with overload only. However, underloads result in further retardation in crack growth rate, which is contrary to the current available achievements.

ACKNOWLEDGEMENTS

The National Natural Science Foundation of China is acknowledged for supporting the project (10802003).

REFERENCES

1. Alcoa Mill Products: 2324 Aluminium Alloy Plate and Sheet; Website (accessed 2009): http://www.alcoa.com/mill_products/catalog/pdf/alloy2324-t39techsheet.pdf
2. Bao R, Zhang X. (2010) *Int J Fatigue* **32**, 1180-1189.
3. S. Beretta, S. Foletti, K. Valiullin. (2010)*Eng Frac Mechanics* **77**, 1835-1848.
4. M. Krkoska, S.A. Barter, R.C. Alderliesten, P. White, R. Benedictus. (2010)*Eng Frac Mechanics* **77**, 1857 - 1865.
5. J. J. Schubbe. (2009)*Eng Fail Anal* **16**, 340-349.
6. J. J. Schubbe. (2009) *Eng Frac Mech* **76**, 1037-1048.
7. Jaap Schijve. (2009). In: *Fatigue of Structures and Materials*, pp.331-335, Springer, Germany.